Biosensors and Bioelectronics 53 (2014) 310–315

Contents lists available at ScienceDirect

Biosensors and Bioelectronics

journal homepage: www.elsevier.com/locate/bios

A novel electrochemical biosensor for sensitive detection of telomerase activity based on structure-switching DNA

Zi Yi [a], Hai-Bo Wang [a], Ke Chen [b], Qing Gao [a], Hao Tang [a,*], Ru-Qin Yu [a], Xia Chu [a,*]

[a] State Key Laboratory of Chemo/Bio-Sensing and Chemometrics, College of Chemistry and Chemical Engineering, Hunan University, Changsha 410082, PR China

[b] College of Chemistry and Chemical Engineering, Hunan Normal University, Changsha 410081, PR China

ARTICLE INFO

Article history:
Received 31 July 2013
Received in revised form
29 September 2013
Accepted 30 September 2013
Available online 14 October 2013

Keywords:
Telomerase
Electrochemical biosensor
Structure-switching DNA probe

ABSTRACT

Telomerase has been considered to be an important tumor biomarker for early cancer diagnostics and a valuable target for therapy treatment. A novel electrochemical biosensor based on structure-switching DNA probe with ferrocene (Fc) as the electroactive reporter to detect telomerase activity was developed. The developed approach displayed desirable dynamic range from 10^2 to 6×10^4 Hela cells mL^{-1} with a detection limit of 100 Hela cells mL^{-1}. This biosensor afforded good reproducibility, stability and simple operations. It provided a useful platform for practical use in quantitative telomerase activity assay for clinical applications. Telomerase inhibitor performance was also investigated and the results indicated the approach was suitable for telomerase inhibitor screening research.

1. Introduction

Human telomerase is a ribonucleoprotein reverse transcriptase which catalyzes the addition of TTAGGG repeats on the telomeric ends of chromosomal DNA from its endogenous RNA template (Bryan and Cech, 1999). As it reported, telomerase has been observed over-expressed in over 85% of all known human tumors and the differential expression between normal somatic cells and cancer cells (Dhaene et al., 2000; Kavaler et al., 1998; Yoshida et al., 1998; Ohuchida et al., 2004; Hirano et al., 1998) makes telomerase a valuable tumor biomarker for early stage cancer diagnosis and an important target for tumor therapy (Shay and Bacchetti, 1997; Shay and Wright, 2002).

Various analytical methods have been developed to detect the activity of telomerase (Hou et al., 2001; Niemeyer et al., 2005; Kim et al., 1994). The PCR-based telomerase repeat extension protocol (TRAP) assay was one of the most frequently used methods (Kim et al., 1994). However, the TRAP method has some limitations, it is inappropriate for the determination of telomerase inhibition (Krupp et al., 1997; Cian et al., 2007), requires expensive equipment and reagents, and is time-consuming. To overcome these shortcomings, several alternative, PCR-free assays for telomerase activity techniques have been developed, such as colorimetric strategy (Xiao et al., 2004b; Fu et al., 2009; Freeman et al., 2010), fluorescence method (Zuo et al., 2011; Ding et al., 2010; Wang et al., 2012), chemiluminescence (Li et al., 2011; Niazov et al., 2004; Pavlov et al., 2004b), electrochemiluminescence (Zhou et al., 2009; Wu et al., 2012), surface Plasmon resonance (Sharon et al., 2010; Maesawa et al., 2003), quartz crystal microbalance (Pavlov et al., 2004a), and electrochemical method (Xiao et al., 2004a; Sato et al., 2005; Eskiocak et al., 2007; Sato and Takenaka, 2012; Shao et al., 2008). These developed approaches provide useful platform for telomerase assay and its related biological research. Nevertheless, each of them still has its disadvantages, such as low sensitivity, complicated manipulation, requiring elaborate instruments or fluorescent probes, and time cost.

Recently, an electrochemical platform using structure-switching DNA probe with certain electroactive reporters for biological analysis has been reported (Zhang et al., 2007; Wu et al., 2007; Liu et al., 2009). This platform, which operates via the alteration of distance of the redox labels from the electrode caused by target induced structure-switching, represent a significant advance of using minimal reagents and working steps, simplified set-up, cost-effective, high sensitivity and excellent compatibility with miniaturization potential.

Inspired by the fact that great distance change between the redox labels and electrode surface could be achieved by using target-induced DNA structure switching approach, we reported for the first time a novel, simple and sensitive electrochemical biosensor for telomerase activity detection utilizing structure-switching DNA probe with ferrocene (Fc) as the electroactive reporter. Scheme 1 illustrates the principle of the approach for telomerase activity assay. Two DNA probes are employed for the

* Corresponding authors. Tel./fax: +86 731 88821916.
E-mail addresses: haotang@hnu.edu.cn (H. Tang), xiachu@hnu.edu.cn, xiachu1972@yahoo.com.cn, xiachu@hnu.cn (X. Chu).

0956-5663/$ - see front matter © 2013 Elsevier B.V. All rights reserved.
http://dx.doi.org/10.1016/j.bios.2013.09.072

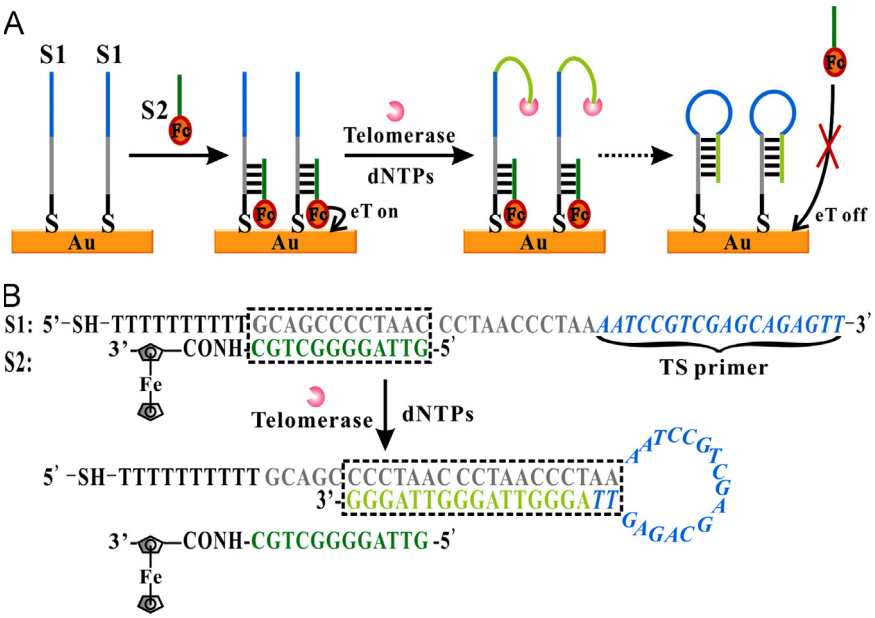

Scheme 1. Illustration of telomerase activity assay based on structure-switching electrochemical biosensor.

structure-switching in this biosensor system. Probe S1 is designed with three segments: the first segment (in blue) is the primer sequence for telomerase; the second segment (in gray) is a recognition region for hybridizing with probe S2 or forming a hairpin structure with its 3′ end after telomerase reaction; and the third segment (in black) is thiolated at the 5-terminus for coating onto gold electrode and has ten thymine bases to maintain proper spatial conformations for promoting the binding efficiency (Schreiner et al., 2010). Probe S2 is a complementary sequence for segment 2 in probe S1 and labeled with Fc tag at the 3′ end. Fc is chosen as the electrochemical signal producer due to its good stability and ease of redox tuning (Zu and Rusling, 1997; D'Souza et al., 2002; Laforge et al., 2004). Firstly, the probe S1 is immobilized on a gold electrode surface via self-assembly through the thiol anchor, then the Fc-labeled probe S2 hybridizes with probe S1, allowing the Fc tag approaching the electrode surface to transfer electrons efficiently. In the presence of telomerase, the telomerase extension occurs at 3′ end of probe S1 by adding the dNTP mixture into solution. The telomerase extension product of probe S1 is folded to form a hairpin structure, leaving only 5 base pairs between probe S1 and probe S2. This structure-switching makes probe S2 unstable at the experimental temperature. As a result, the Fc-labeled probe S2 is released from the electrode surface with a substantially decreased redox current attributed to the increased electron-tunneling distance. This design affords a simple and rapid operation, excellent stability and high sensitivity for telomerase activity detection, and the strategy could be implemented with minimized reagents and working steps.

2. Experimental

2.1. Reagents and materials

All oligonucleotides used in this work were synthesized by Takara Biotechnology Co. Ltd. (Dalian, China). The sequences of the oligonucleotides were given in Table S1 (in Supplemetary materials). Thermodynamic parameters and secondary structures of both oligonucleotides were calculated using bioinformatics software (http://mfold.rna.albany.edu/). HeLa cells, PC-3 cells (Human prostate epithelial tumor cells), K562 cells (Human leukemia chronic cell lines), U937 cells (Human leukemia mononuclear acute cell lines), MDA-MB-231 cells (Human breast carcinoma cell lines), HEK-293 T cells (Human embryonic kidney cells) were obtained from American Type Culture Collection (ATCC, Manassas, VA).

Ferrocenecarboxylic acid (Fc), 1-ethyl-3-(3-dimethyl-aminopropyl) carbodiimide hydrochloride (EDC), and N-hydroxysulfosuccinimide (Sulfo-NHS) were all purchased from Sigma-Aldrich Chemical Co. 4-(2-Aminoethyl) benzenesulfonyl fluoride hydrochloride (AEBSF) and Nonidet-P 40 (NP-40) were purchased from Bio Basic.Inc. Sodium deoxycholate, Tris, diethyl pyrocarbonate (DEPC) was obtained from the Sinopharm Chemical Reagent Co., Ltd. (Shanghai, PRC). 5 × TBE buffer was purchased from Sangon Biotech Co., Ltd. (Shanghai). All solutions were prepared using ultrapure water, which was obtained through a Millipore Milli-Q water purification system (Billerica, MA) and had an electrical resistance of >18.3 MΩ.

2.2. Preparation of Fc-labeled oligonucleotides

The Fc label was conjugated to the 3′ NH_2-moiety oligonucleotide probe S2, using the succinimide coupling (EDC-NHS) method (Zhang et al., 2007, 2009; Fahlman and Sen, 2002; Huang et al., 2009). In brief, 100 μL of 10 μM oligonucleotide probe S2 was mixed with 100 μL of 10 mM PBS (pH 7.4) containing 10 mM ferrocenecarboxylic acid, 1 mM EDC, and 5 mM Sulfo-NHS, followed by incubation for 2 h at 37 °C. The conjugate was dialyzed against 10 mM PBS (500 mL) for 24 h to remove excessive ferrocenecarboxylic acid. The resulting solution was stored at −20 °C before use.

2.3. Cell culture

HeLa cells, K562 cells and U937 cells were all cultured in RPMI 1640 medium supplemented with 10% fetal bovine serum (FBS) and 100 IU mL^{-1} of penicillin–streptomycin. PC-3 cells were cultured in F-12 K medium. MDA-MB-231 cells and HEK-293 T cells were grown in DMEM supplemented with 10% fetal calf serum. The cells were maintained at 37 °C in a humidified atmosphere (95% air and 5% CO_2) and were kept in logarithmic growth phase by routine passage every 2–3 days. The cancer cell densities

were determined by using a hemocytometer, and this was performed prior to any experiments.

2.4. Telomerase extraction

The telomerase was extracted by the NP-40 method according to a documented protocol (Maesawa et al., 2003). HeLa cells were removed from the substrate by trypsinization, washed twice with PBS (pH 7.4) and centrifugated at 3000 rpm for 5 min at 4 °C. The cells was resuspended in 200 μL of ice cold lysis buffer (10 mM Tris–HCl, 1% NP-40, 0.25 mM sodium deoxycholate, 10% glycerol, 150 mM NaCl, 0.1 mM AEBSF, pH 8.0) by retropipeting at least three times at a concentration of 1.0×10^7 cells mL^{-1}, kept on ice for 30 min and then centrifugated at 12,000 rpm for 20 min at 4 °C. The resulting extracts were flash frozen in liquid nitrogen at −80 °C for further experiment.

2.5. Gold electrode treatment and oligonucleotide immobilization

Prior to the experiment, the working gold electrodes (~2 mm diameter, 99.99% polycrystalline, CH Instrument Inc.) were first immersed in piranha solution (H_2SO_4/H_2O_2=3:1 in volume) for 3 h, polished carefully with 0.05 μm Al_2O_3 powder on fine chammy skin for 5 min, and then sonicated in absolute ethanol and ultrapure water for 3 min twice to remove the possible bound microparticles. Finally, the electrode was again rinsed thoroughly with ultrapure water and dried in nitrogen stream.

The pretreated gold electrode was immersed in a solution containing 1 μM thiolated probe S1 in 10 mM Tris–HCl buffer (1.0 M NaCl, pH 8.0) for 12 h at 4 °C. This process produced a self-assembly monolayer (SAM) of thiolated oligonucleotide on the electrode surface. Then, the electrode was rinsed thoroughly with 10 mM Tris–HCl buffer (pH 8.0) containing 1.0 M NaCl for 10 min. The resulting thiolated oligonucleotide functionalized electrode was subsequently incubated with 50 μL hybridization buffer solution (10 mM PB, 1.0 M NaCl, pH 7.4) containing 1.0 M ferrocene-tagged S2 for 4 h at 49 °C. The electrode was then rinsed with 10 mL mixture solution of 1 mL 10 × TRAP reaction buffer (200 mM Tris–HCl, 15 mM $MgCl_2$, 630 mM KCl, pH 8.3), 1 mL NP-40 lysis buffer (10 mM Tris–HCl, 1% NP-40, 0.25 mM sodium deoxycholate, 10% glycerol, 150 mM NaCl, 0.1 mM AEBSF, pH 8.0) and 8 mL DEPC water at a room temperature for three times. The sensor thus obtained was stored at 4 °C in PBS buffer and was found to maintain the activity for more than 1 week.

2.6. Electrochemical detection of telomerase activity

The pretreated electrode was immersed in 60 μL of extension solution with 6.0 μL various concentration of telomerase extracts, 6.0 μL of 10 × TRAP reaction buffer, 1.2 μL of 10 mM dNTP mixture (dATP, dCTP, dGTP, dTTP) and 46.8 μL of DEPC water at 30 °C for 2 h. The electrode was then rinsed with 10 mL mixture solution of 1 mL 10 × TRAP reaction buffer, 1 mL NP-40 lysis buffer and 8 mL DEPC water at room temperature (~25 °C) for 10 min. For control experiments, telomerase extracts were pretreated heat treated (90 °C for 30 min). In the inhibition experiments, different volumes of 3′-azido-3′-deoxythymidine (AZT) solution (Sigma Aldrich Inc.) were pre-incubated with 6.0 μL 10 × TRAP reaction buffer, 1.0 μL telomerase extracts and DEPC water at 37 °C for 1.5 h, and the telomerase extension reaction was then performed at 30 °C for 2 h.

All electrochemical measurements including differential pulse voltammetry (DPV), cyclic voltammetry (CV), and electrochemical impedance spectroscopy (EIS) were performed on an electrochemical analyzer CHI-660 A (CH Instruments, Shanghai, China) at room temperature (~25 °C). A three-electrode system consisting of a KCl saturated calomel reference electrode (SCE), a platinum counter electrode and the working electrode (gold electrode) was used. DPV was recorded in a 1/15 M PB (pH 7.4) solution containing 0.3 M NaCl and 0.1 M $KClO_4$ at a potential range from 0 to 0.5 V with a modulation amplitude of 25 mV and a scan rate of 10 mV/s. CV was performed at a potential range from −0.1 V to 0.5 V in a 1/15 M PB (pH 7.4) solution containing 0.3 M NaCl and 0.1 M $KClO_4$. EIS was performed in 1/15 M PB (pH 7.4) containing 5 mM $Fe(CN)_6^{3-/4-}$ (1:1 mixture) and 0.1 M KCl in the frequency range from 0.1 Hz to 100 kHz with 5 mV as the amplitude at a bias potential of −0.19 V (vs. SCE) with frequency modulation of 5 mV. The reported DPV curves were background subtracted through extrapolation to the baseline in the regions far from the peaks.

2.7. Gel electrophoresis

The prepared sample mixed with bromophenol blue was analyzed using gel electrophoresis in 4% (w/w) agarose containing 0.5 × TBE electrophoresis buffer. Electrophoresis was performed at a constant potential of 100 V for 90 min with loading each sample into the lanes. The gels were dried on filter paper and visualized using a Tocan 240 gel imaging system (Shanghai Tocan Biotechnology Company).

3. Results and discussion

3.1. CV and DPV performance of different modified electrodes

The proposed electrochemical biosensor for telomerase was first characterized by cyclic voltammetry (CV) and Differential pulse voltammetry (DPV) as shown in Fig. 1. It was observed in Fig. 1A, when Fc-labled probe S2 was hybridized with probe S1 modified on the electrode, in the absence of telomerase, a couple of strong redox peaks appeared at 0.136 and 0.335 V (vs. SCE) in CV (curve a), indicating electrochemical characteristics of Fc at electrode surface. While in the presence of high telomerase concentration (~6×10^4 Hela cells mL^{-1}), the couple of redox peaks almost disappeared (curve b). Those observations implied that the biosensor was sensitively responsive to telomerase. Control experiment by incubating the probe S1 and S2 modified electrode with heat-treated telomerase indicated the inactive telomerase had negligible effect on redox peak (curve c). Further control experiment was using two control DNA probes: thiolated probe S3 and Fc-labeled probe S4 modified electrode incubating with active telomerase concentration (~6×10^4 Hela cells mL^{-1}), the the results revealed that the redox peak of the Fc nearly did not change (curve d). Fig. 1B shows similar results but with better resolution of these observations in DPV measurements. These results demonstrated that the extension reaction of telomerase induced the folding of the probe S1 into a hairpin structure, which resulted in the release of the Fc-labeled probe S2 from the electrode surface with a substantially decreased redox current. And the present approach had good selectivity with active telomerase.

3.2. Gel electrophoresis characterization of the assay

To further verify the mechanism of the assay, we designed two DNA probes, probe S5 and FAM-labeled probe S6 (see Table S1 in Supplementary materials for their sequences), for agarose gel electrophoresis experiments. Probe S5 had same sequence with probe S1 but without thiolation at 5′ end while Probe S6 had same sequence with probe 2 and labeled with FAM. Fig. S1 (in Supplementary materials) illustrates different migration of these DNA probes under different conditions. A bright band was obtained on

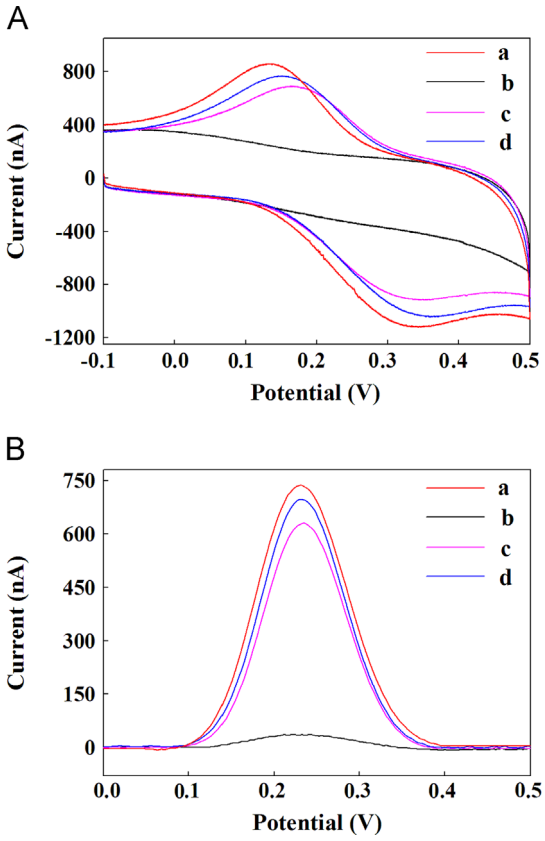

Fig. 1. Typical CV (A) and DPV (B) curves of the structure-switching electrochemical biosensor with differently modified gold electrodes: (a) probe S1+Fc-labeled probe S2+NP-40 lysis buffer solution, (b) probe S1+Fc-labeled probe S2+active telomerase Hela cell extracts, (c) probe S1+Fc-labeled probe S2+heat-treated telomerase Hela cell extracts, (d) probe S3+Fc-labeled probe S4+active telomerase Hela cell extracts.

the gel at about 12 bp corresponding with FAM-labeled probe S6 (lane 1). After incubating probe S6 with the complementary DNA probe S5, a bright bane was obviously observed at nearly 50 bp on the gel which validated the hybridization process (lane 2). To obtain better image and further evidence, we added SYBR Green I, which could be embedded into the double-stranded DNA and provide brighter image for telomerase treatment experiments. When incubated with active telomerase, several bands with decreased migration shifts (>50 bp) indicated various DNA length products from telomerase extension, while the band in 12 bp positions corresponding with FAM-labeled probe S6 gave direct evidence that the hybridized probe S6 became unstable and was released due to the telomerase extension and structure-switching (lane 3). When incubating with heat-treated telomerase, same position at 50 bp but brighter image obtained (lane 4 compared with lane 2) indicated the heat-treated telomerase lost its activity.

3.3. Electrochemical characterization of the biosensor

To investigate the surface interactions, electrochemical impedance spectroscopy (EIS) was performed. Fig. S2 shows the impedance spectra in the form of a Nyquist plot. The bare gold electrode behaved as an ideal conductor and the impedance spectra gave a linear plot (curve a). The probe S1 modified electrode exhibited much larger impedance than the bare electrode (curve b), due to the formation of a barrier for the electron transfer at the electrode interface. After hybridization with Fc-labeled probe S2, the electrochemical impedance greatly decreased (curve c). This exhibited facilitated electron transfer kinetics because of the surface confinement of the Fc labels. In the presence of telomerase, the resistance increased substantially again due to the release of Fc labels (curve d).

In addition, the electrochemical process on electrode surface was also investigated by cyclic voltammetry experiments. As shown in Fig. S3A (in Supplementary materials), after Fc-labeled probe S2 hybridized with probe S1 modified at electrode, the CV peak current were obtained at varying potential scanning rates. Fig. S3B (in Supplementary materials) also showed that the reduction peak currents of the sensor were observed increase to in linear correlation to the scan rate in the range of 10–120 mV/s. These observations manifested that the sensor demonstrated typical surface-bound electrochemical processes and the Fc tags were confined to the electrode surface.

3.4. Optimization of experimental conditions

For the developed biosensor, probe S1 was hybridized with Fc-labeled probe S2, to maximize the efficiency of hybridization, several parameters were optimized. The hybridization reaction time and hybridization reaction temperature were first investigated. Fig. S4A and B (in Supplementary materials) depicts typical DPV peak current responses in correlation to the two assay conditions in hybridization reaction, respectively. It was observed in Fig. S4A that with the increased of hybridization reaction time, DPV peak current intensities in assay were enhanced substantially at first, and then became flat when the time was longer than 4 h. And DPV peak current intensities reached its maximum only when the hybridization reaction temperature at 49 °C in Fig. S4B. Therefore, 4 h of the hybridization reaction time and 49 °C of the hybridization reaction temperature were taken throughout the subsequent experiments. The telomerase extension reaction was performed after the hybridization reaction, in which the elongated DNA probe occurred structure-switching, resulting in the releasing of the Fc-labeled probe S2. Hence, to obtain a maximal DPV signal change, the concentration of Mg^{2+} in telomerase extension reaction buffer and the time of telomerase extension reaction were then investigated. As shown in Fig. S4C in Supplementary materials, DPV peak current value decreased first to a minimum at the Mg^{2+} concentration of 1.5 mM, and then increased again with the increasing of Mg^{2+} concentration. This phenomenon might be due to the fact that the DNA double strand was so stable at high Mg^{2+} concentration that the releasing of the Fc-labeled probe S2 became difficult. In addition, it can be seen from Fig. S4D in Supplementary materials that as the time of telomerase extension reaction increased, the DPV peak current intensities declined gradually, and became almost leveled off for 120 min. As a result, 1.5 mM of Mg^{2+} concentration and 120 min of telomerase extension reaction time was used throughout subsequent experiments.

3.5. Electrochemical detection of telomerase activity

The ability of quantitative analysis of telomerase was investigated by performing telomerase extracts from various concentrations of Hela cells under the optimal experimental conditions. Fig. 2 shows a dynamic correlation between DPV peak current at 0.232 V and telomerase activity from 10^2 to 6×10^4 Hela cells mL^{-1}. The concentration response was quantified by observing the change in the area of the DPV peak at 0.232 V, which was plotted in Fig. 2B. In Fig. 2C, the peak currents exhibited a linear correlation to the logarithm of the Hela cell concentration across the range from 10^2 cells to 6×10^4 cells. The linear regression equation was I_p (nA) = 1243 − 259.7l gC (cell number/mL) (where I_p was the peak current, and C was the Hela cell concentration) with a correlation coefficient of 0.9865. A high-dose sensitivity was also obtained in this five-decade cell number range with a detection

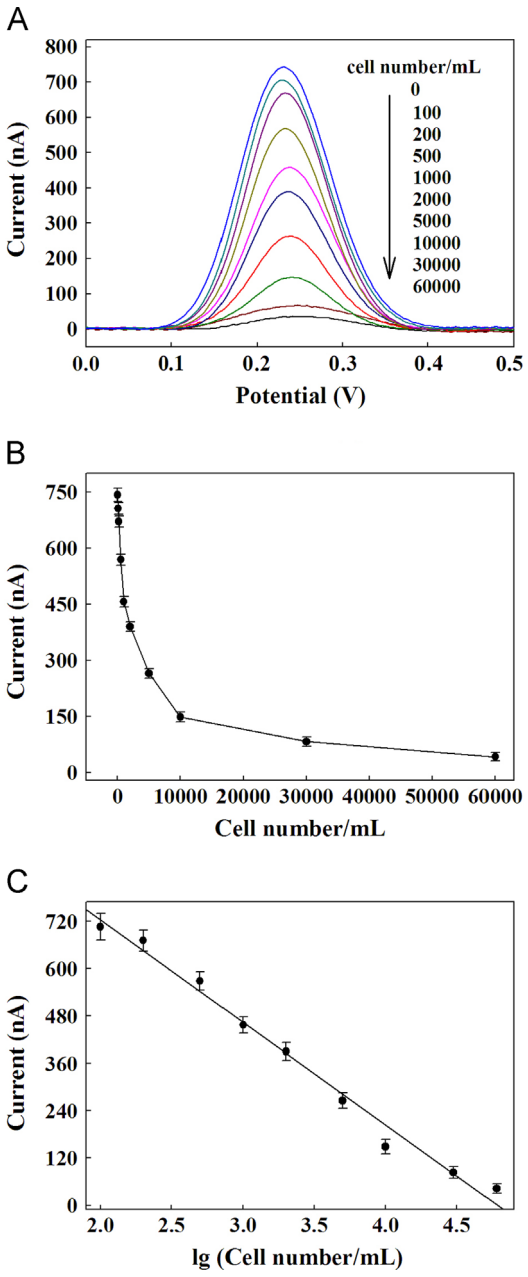

Fig. 2. (A) Typical DPV response curves in response to telomerase extracts from different concentrations of HeLa cells. (B) The plot of DPV peak currents vs. Hela cells concentrations. (C) Corresponding DPV peak currents vs. the logarithm of the Hela cell concentrations. The error bars represented RSD across three repetitive experiments.

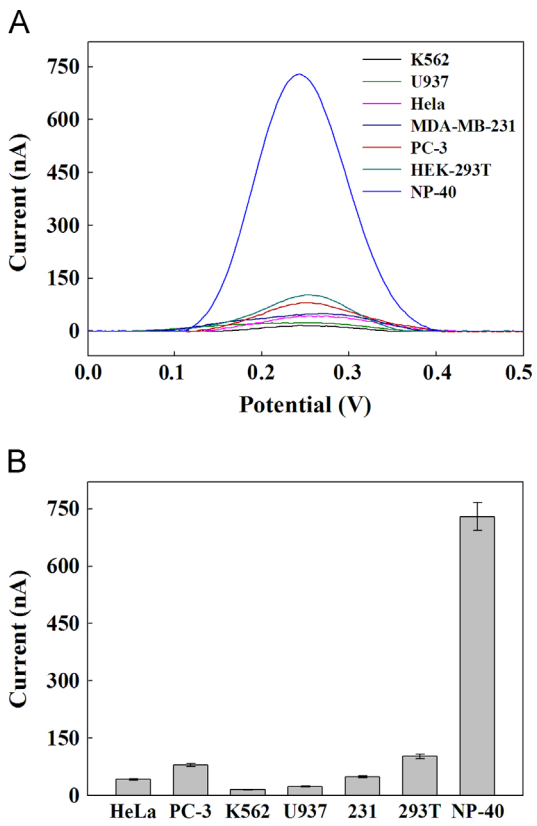

Fig. 3. (A) Normalized DPV peak currents in response to different cancer cells. DPV was recorded in 1/15 M PB buffer (pH 7.4) containing 0.3 M NaCl and 0.1 M $KClO_4$ within the potential range from 0 to 0.5 V. (B) The histogram of DPV peak currents vs. different cancer cells.

limit of 100 Hela cells mL^{-1} as calculated in terms of the rule of 3 times standard deviation over the blank response. Compared with the sensors reported by other groups (Li et al., 2011; Pavlov et al., 2004a, 2004b; Sato et al., 2005; Shao et al., 2008), the developed sensor exhibited a relatively high sensitivity for the detection of telomerase activity. Additionally, the present strategy possessed excellent reproducibility. Relative standard deviations (RSDs) of peak current intensities were 4.8%, 3.1% and 4.5% in three repetitive assays of 200, 2000 and 10,000 Hela cells. The stability of the sensor was also studied under continuous linear scans for 10 cycles, and the results indicated that the developed sensor had excellent stability. Moreover, we analyzed the performance of the oligonucleotide-immobilized electrode before and after being stored at 4 °C in PBS buffer for 1 week, and the results indicated that the performance of the sensor remained unchanged in 1 week (see Fig. S5 in Supplementary materials).

The developed electrochemical biosensor was then applied for detecting telomerase activity with different cancer cells. Five types of cancer cells (PC-3 cell, K562 cell, U937 cell, MDA-MB-231 (231) cells and HEK-293T (293T) cells) were selected to extract telomerase, then, each extracts was individually added to the reaction solution, and the DPV response was recorded after incubation at 30 °C for 2 h. As shown in Fig. 3, the sensor showed significant DPV peak current decrease in response to telomerase extracts of all types of cancer cells (include Hela cell), compared to the peak current when incubated only with NP-40 lysis buffer. These results were consistent with the previous reports that the telomerase could be detected in nearly 85% of human cancer cells.

3.6. *Inhibition characterization of telomerase activity*

The inhibition of telomerase activity was investigated by adding varying concentration of 3′-azido-3′-deoxythymidine (AZT), a recognized inhibitor of telomerase enzymatic activity (Melana et al., 1998; White et al., 2001), to the solution in the telomerase extension reaction step. The telomerase initially added to the assay were extracted from 1×10^4 HeLa cells, and the concentration of AZT used was from 10 to 40 mM. DPV peak currents showed increased signal intensity as a function of increased AZT concentrations (Fig. 4A). The corresponding histogram of DPV peak currents vs. the AZT concentrations is also shown in Fig. 4B. These results suggested the potential use of our assay for telomerase inhibition study.

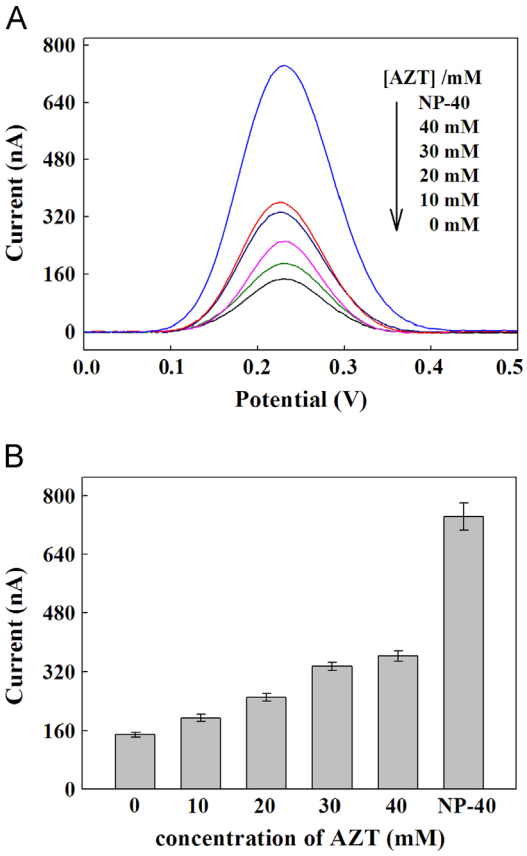

Fig. 4. (A) DPV response curves at various AZT concentrations after pre-incubation with telomerase extracts at 37 °C for 1.5 h. (B) The histogram of DPV peak currents vs. the AZT concentrations.

4. Conclusions

We have developed a novel electrochemical biosensor for the sensitive telomerase activity detection based on structure-switching DNA probe. This method exhibited a very broad linear response range and high sensitivity, excellent stability and reproducibility as well as simple operations. In view of the advantages this approach was hold great potential for telomerase activity detection and its inhibitor screening research.

Acknowledgments

This work was supported by the National Natural Science Foundation of China (No. 21275045), NCET-11-0121, and Hunan Provincial Natural Science Foundation of China (Grant 12JJ1004).

Appendix A. Supplementary material

Supplementary data associated with this article can be found in the online version at http://dx.doi.org/10.1016/j.bios.2013.09.072.

References

Bryan, T.M., Cech, T.R., 1999. Cell Biol. 11, 318–324.
Cian, A.D., Cristofari, G., Reichenbach, P., Lemos, E.D., Monchaud, D., Teulade-Fichou, M.-P., Shi-ya, K., Lacroix, L., Lingner, J., Mergny, J.-L., 2007. PNAS 104, 17347–17352.
D'Souza, F., Zandler, M.E., Smith, P.M., Deviprasad, G.R., Arkady, K., Fujitsuka, M., Ito, O., 2002. J. Phys. Chem. 106, 649–656.
Dhaene, K., Marck, E.V., Parwaresch, R., 2000. Virchows Arch. 437, 1–16.
Ding, C.F., Li, X.L., Ge, Y., Zhang, S.S., 2010. Anal. Chem. 82, 2850–2855.
Eskiocak, U., Ozkan-Ariksoysal, D., Ozsoz, M., Öktem, H.A., 2007. Anal. Chem. 79, 8807–8811.
Fahlman, R.P., Sen, D., 2002. J. Am. Chem. Soc. 124, 4610–4616.
Freeman, R., Sharon, E., Teller, C., Henning, A., Tzfati, Y., Willner, I., 2010. ChemBioChem 11, 2362–2367.
Fu, R.Z., Li, T.H., Prak, H.G., 2009. Chem. Commun. 39, 5838–5840.
Hirano, Y., Fujita, K., Suzuki, K., Ushiyama, T., Ohtawara, Y., Tsuda, F., 1998. Cancer 83, 772–776.
Hou, M., Xu, D.W., Björkholm, M., Bruber, A., 2001. Clin. Chem. 47, 519–524.
Huang, Y., Zhang, Y.L., Xu, X.M., Jiang, J.H., Shen, G.L., Yu, R.Q., 2009. J. Am. Chem. Soc. 131, 2478–2480.
Kavaler, E., Landman, J., Chang, Y.L., Droller, M., Liu, B.C.-S., 1998. Cancer 82, 708–714.
Kim, N.W., Platyszek, M.A., Prowse, K.R., Harley, C.B., West, M.D., Ho, P.L.C., Coviello, G.M., Wright, W.E., Weinrich, S.L., Shay, J.W., 1994. Science 266, 2011–2015.
Krupp, G., Kühne, K., Tamm, S., Klapper, W., Heidorn, K., 1997. Nucleic Acids Res. 25, 919–921.
Laforge, F.O., Kakiuchi, T., Shigematsu, F., Mirkin, M.V., 2004. J. Am. Chem. Soc. 126, 15380–15381.
Li, Y., Li, X., Ji, X.T., Li, X., 2011. M. Biosensors Bioelectron. 26, 4095–4098.
Liu, S.J., Nie, H.G., Jiang, J.H., Shen, G.L., Yu, R.Q., 2009. Anal. Chem. 81, 5724–5730.
Maesawa, C., Inaba, T., Sato, H., Iijima, S., Ishida, K., Terashima, M., Sato, R., Suzuki, M., Yashima, A., Ogasawara, S., Oikawa, H., Sato, N., Siatio, K., Masuda, T., 2003. Nucleic Acids Res. 31, 4e.
Melana, S.M., Holland, J.F., Pogo, B.G.-T., 1998. Clin. Cancer Res. 4, 693–696.
Niazov, T., Pavlov, V., Xiao, Y., Gill, R., Willner, I., 2004. Nano Lellers 4, 1683–1687.
Niemeyer, C.M., Adler, M., Wacker, R., 2005. Trends Biotechnol. 23, 208–216.
Ohuchida, K., Mizumoto, K., Ishikawa, N., Sato, N., Nagai, E., Yamaguchi, K., Takaishi, H., Ide, T., Tanaka, M., 2004. Cancer 101, 2309–2317.
Pavlov, V., Willner, I., Dishon, A., Kotler, M., 2004a. Biosensors Bioelectron. 20, 1011–1021.
Pavlov, V., Xiao, Y., Gill, R., Dishon, A., Kotler, M., Willner, I., 2004b. Anal. Chem. 76, 2152–2156.
Sato, S., Kondo, H., Nojima, T., Takenaka, S., 2005. Anal. Chem. 77. (7394–7309).
Sato, S., Takenaka, S., 2012. Anal. Chem. 84, 1772–1775.
Schreiner, S.M., Shudy, D.F., Hatch, A.L., Opdahl, A., 2010. Anal. Chem. 82, 2803–2810.
Shao, Z.Y., Liu, Y.X., Xiao, H., Li, G.X., 2008. Electrochem. Commun. 10, 1502–1504.
Sharon, E., Freeman, R., Riskin, M., Gil, N., Tzfati, Y., Willner, I., 2010. Anal. Chem. 82, 8390–8397.
Shay, J.W., Bacchetti, S., 1997. Eur. J. Cancer 33, 787–791.
Shay, J.W., Wright, W.E., 2002. Cancer Cell 2, 257–265.
Wang, H.B., Wu, S., Chu, X., Yu, R.Q., 2012. Chem. Commun. 48, 5916–5918.
White, L.K., Wright, W.E., Shay, J.W., 2001. Trends Biotechnol. 19, 114–120.
Wu, L., Wang, J.S., Feng, L.Y., Ren, J.S., Wei, W.L., Qu, X.G., 2012. Adv. Mater. 24, 2447–2452.
Wu, Z.S., Guo, M.M., Zhang, S.B., Chen, C.R., Jiang, J.H., Shen, G.L., Yu, R.Q., 2007. Anal. Chem. 79, 2933–2939.
Xiao, Y., Pavlov, V., Gill, R., Bourenko, T., Willner, I., 2004a. ChemBioChem 5, 374–379.
Xiao, Y., Pavlov, V., Tamara, N., Dishon, A., Kotler, M., Willner, I., 2004b. J. Am. Chem. Soc. 126, 7430–7431.
Yoshida, K., Sakamoto, S., Sumi, S., Higashi, Y., Kitahara, S., 1998. Cancer 83, 760–766.
Zhang, Y.L., Huang, Y., Jiang, J.H., Shen, G.L., Yu, R.Q., 2007. J. Am. Chem. Soc. 129, 15448–15449.
Zhang, Y.L., Wang, Y., Wang, H.B., Jiang, J.H., Shen, G.L., Yu, R.Q., 2009. Anal. Chem. 81, 1982–1987.
Zhou, X.M., Xing, D., Zhu, D.B., Li, J., 2009. Anal. Chem 81, 255–261.
Zu, X., Rusling, J.F., 1997. Langmuir 13, 3693–3699.
Zuo, X.L., Xia, F., Patterson, A., Soh, H.T., Xiao, Y., Plaxco, K.W., 2011. ChemBioChem 12, 2745–2747.